Hindawi
Advances in Materials Science and Engineering
Volume 2019, Article ID 2646012, 9 pages
https://doi.org/10.1155/2019/2646012

Research Article

Mechanical and Self-Sensing Properties of Multiwalled Carbon Nanotube-Reinforced ECCs

Chuanbo Liu,[1] Guozhen Liu,[2] Zhi Ge,[3] Yanhua Guan,[3] Zhiyong Cui,[4] and Jian Zhou[3]

[1]*Jinan Highway Administration, Jinan 2500123, China*
[2]*Zhangqiu Highway Administration, Jinan 250200, China*
[3]*School of Qilu Transportation, Shandong University, Jinan 250002, China*
[4]*Taian Department of Transportation, Taian 271000, China*

Correspondence should be addressed to Zhi Ge; zhige@sdu.edu.cn

Received 2 February 2019; Revised 17 April 2019; Accepted 9 May 2019; Published 3 June 2019

Guest Editor: Young H. Kim

This paper investigates the effect of type and dosage of multiwalled carbon nanotubes (MWCNTs) on the mechanical and self-sensing properties of engineered cementitious composites (ECCs). Two types of MWCNTs (MWCNTa and MWCNTb) were employed. The tensile and flexural strengths of CNT-reinforced ECCs were improved compared with normal ECCs, while the ultimate tensile strain and midspan deflection were reduced. Compared with the dosage of MWCNTs, the type had less effect on these properties. The percolation threshold was around 0.3 wt.%. ECCs containing MWCNTs had good self-sensing ability under different loading conditions. When the midspan deflection increased from 0.1 to 0.6 mm, the fractional change in resistivity reached 9%. The dosage of MWCNTs had a significant effect on the self-sensing ability. As the MWCNT content increased, the amplitude of fractional change in resistivity decreased.

1. Introduction

Concrete structures deteriorate during their service life because of continuous use, environment, difficulties in proper inspection methods, lack of maintenance, etc. Therefore, structural health monitoring (SHM) is critical because of the huge loss of life and property caused by structural failure. One of the key components of SHM is data acquisition. Currently, sensors are used to collect strain, temperature, stress, etc. However, these sensors have disadvantages of high cost, loss of mechanical properties in structure, and poor durability [1, 2]. Self-sensing materials on the other hand could overcome the drawbacks of traditional sensors and be used for data collection because they are structural materials themselves and able to sense their own strain and damage [3]. Currently, carbon nanofibres (CNFs), carbon nanotubes (CNTs), and graphite nanoplatelets (GNPs) are incorporated into cementitious materials to produce intrinsic self-sensing cementitious materials to develop self-sensing cement composites. Currently, most studies focus on type and dosage of additives, mixing method, and self-sensing ability of materials or structures [1–10]. Studies show that the resistivity and piezoresistivity of the CNT-cement composite depend on the conductivity network in the composite. Different optimal dosages of CNTs for better sensing abilities were reported. For example, Han et al. [5] found that composites with 0.1 wt.% CNTs had better performance. However, Luo et al. [6] concluded that 0.5 wt.% of CNTs showed better stability. Dispersion of CNTs will also affect the properties of the CNT-cement composite. In order to achieve improved mechanical and electrical properties, the CNTs should be dispersed effectively in the cement paste. Al-Dahawi et al. [10] investigated the effect of different dispersion methods on the electrical resistivity and found that mechanical mixing with shear effect was very influential in dispersing CNTs. Currently, most studies used cement. However, traditional cement-based materials are typically quasi-brittle material with low tensile strain capacity. In this case, it is impossible

to monitor large deformation of the structure by these self-sensing cement composites.

Engineered cementitious composites (ECCs) are fiber-reinforced cementitious composites with excellent tensile ductility and good durability under harsh environment [11–19]. The research found that incorporating conductive filler into ECCs could make it self-sensing [18–23]. Lin et al. found that adding a small dosage of carbon black (CB) into the ECC system could enhance matrix tensile strength and achieve self-sensing ability [20]. Al-Dahawi et al. [21] found the percolation threshold of multiwalled carbon nanotubes, graphene nanoplatelets, carbon black, and carbon fiber in ECCs was around 0.55%, 2.00%, 2.00%, and 1.00%, respectively. These carbon-based materials improved compressive strength and self-sensing ability under both compressive and flexural tests [22]. Current research shows that it is possible to use modified ECCs for SHM. However, few research was conducted to investigate the influence of types of CNTs on the mechanical and self-sensing properties of CNT-reinforced ECCs at different midspan deflection ranges. In this study, the uniaxial tensile test and four-point flexural test were employed to study the mechanical and self-sensing ability of ECCs containing different dosages and types of CNTs.

2. Experimental Work

2.1. Materials. The P.O. 42.5 ordinary Portland cement and Class F fly ash, produced in Jinan, China, were used. The main chemical compositions are presented in Table 1. The 0.096–0.18 mm sand was local silica sand. The polyvinyl alcohol (PVA) fiber had a length of 12 mm, diameter of 39 mm, nominal tensile strength of 1620 MPa, specific gravity of 1.3, and elastic modulus of 42.8 GPa. Figure 1 shows the microstructure of PVA fiber. Two types of multiwalled carbon nanotubes were adopted. The main properties are summarized in Table 2. The surfactant for the dispersion of MWCNTs was polyvinylpyrrolidone (PVP), a white powder produced in Jinan. The polycarboxylate-based high-range water reducer (HRWR) was employed. The water used was distilled water produced in the laboratory.

2.2. Preparation of ECC Specimen. The uniform dispersion of MWCNTs without agglomerations is critical for specimen's mechanical properties and electrical conductivity by forming continuous conductive network [10, 24]. In this study, PVP (PVP to MWCNT ratio of 0.8) was first added into the distilled water and then stirred using a magnetism stirrer until fully dissolved. Subsequently, MWCNTs were added into the solution and sonicated with a probe sonicator (Ningbo Scientz Biotechnology, Model JY92-IIN, 640 W ultrasonic power and 40% amplitude) for 15 minutes.

To prepare the specimen, the cement, fly ash, and sand were first mixed at low speed (140 rpm) for 2 minutes. The HRWR was added into the well-dispersed MWCNT solution and then poured into the mixer. All materials were mixed at low speed for 1 minute, followed by 2 minutes at high speed (285 rpm). After that, the PVA fibers were slowly added into the mix and continuously mixed at high speed for three more minutes to ensure uniform dispersion of the PVA fibers. After mixing, the mix was poured into the mold. The specimens were demolded after 1 day and cured at a standard curing room with a temperature of $22 \pm 2^{\circ}$C and relative humidity of 98% for 28 days.

Table 1: Main chemical compositions of cement and fly ash.

Composition (%)	CaO	SiO_2	Al_2O_3	MgO	Fe_2O_3	SO_3	Na_2O
Cement	64.63	21.96	4.73	2.59	0.03	0.3	0.56
Fly ash	3.88	45.66	31.52	0.89	9.70	0.37	3.02

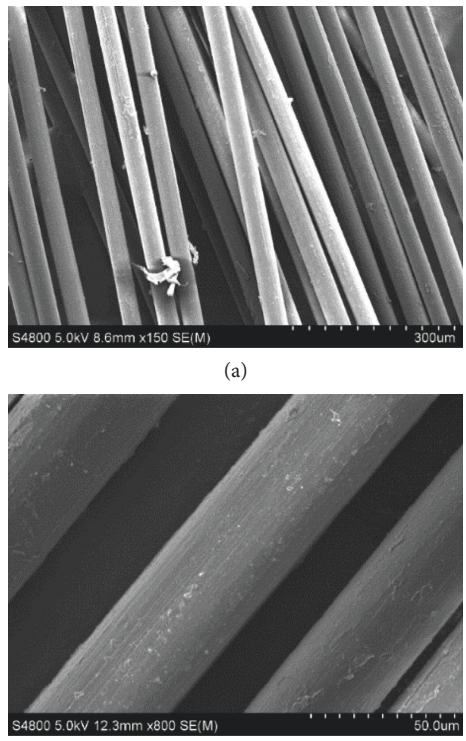

Figure 1: Microstructure of PVA fiber.

2.3. Experimental Design. This paper studied the effect of MWCNT type and dosage on the mechanical and self-sensing properties. Two types of MWCNTs (MWCNTa and MWCNTb) and four dosage levels were adopted. Therefore, total 9 mixes were designed. The different mix proportions are listed in Table 3. In all mixes, the PVP to MWCNT ratio was 0.8. Different amount of HRWR was used for different mixes to achieve similar workability of ECC mortar (before adding fiber) because workability of the matrix significantly influences fiber dispersion uniformity, which results in different strain capacities [25].

2.4. Testing Methods. Uniaxial tensile and four-point bending tests were conducted to evaluate the strain-hardening property of ECCs. For each test, three $5\,\text{mm} \times 50\,\text{mm} \times 170\,\text{mm}$ specimens were used. The average

Table 2: Main physical properties of MWCNTs.

Type	OD (nm)	Length (μm)	Purity (wt.%)	Ash (wt.%)	−COOH (wt.%)	Specific surface area ($m^2 \cdot g^{-1}$)
MWCNTa	8–15	~50	>95	<1.5	2.56	>130
MWCBTb	30–50	<10	>98	<1.5	0.73	>100

Table 3: Mix proportions of MWCNT-reinforced ECCs.

No.	Normal ECC mix proportions						MWCNTs (wt.%)	
	Cement (kg/m^3)	Fly ash (kg/m^3)	Sand (kg/m^3)	Water (kg/m^3)	HRWR (kg/m^3)	Fiber (kg/m^3)	MWCNTa	MWCNTb
1	570	684	455	331	5.5	27	0	0
2	570	684	455	331	7	26	0.1	0
3	570	684	455	331	8.5	26	0.3	0
4	570	684	455	331	10	26	0.5	0
5	570	684	455	331	12	26	0.7	0
6	570	684	455	331	6.5	26	0	0.1
7	570	684	455	331	7	26	0	0.3
8	570	684	455	331	7.5	26	0	0.5
9	570	684	455	331	8	26	0	0.7

value was presented. For direct tensile testing, the LVDT displacement sensor was employed to measure displacement. The load was applied at 0.2 mm/min by the WDW-100E universal testing machine (Figure 2(a)).

The bending test could be used as an indirect evaluation method for the strain-hardening properties of ECCs. The 15 mm × 50 mm × 170 mm specimen was loaded at 0.5 mm/min using the WDW-100E universal testing machine (Figure 2(b)). The midspan deflection was monitored by the LVDT displacement sensor.

The two-probe method was adopted to measure the electrical resistivity of the ECC specimen (Figure 3). The voltage between two electrodes (70 mm apart) was automatically measured by using a Keithley 2100 multimeter. The electrical resistance was calculated by Ohm's law. The electrical resistivity (ρ) and the fractional change in resistivity were calculated by using the following equations:

$$\rho = R\frac{A}{l}, \qquad \frac{\Delta\rho}{\rho_0} = \frac{\rho_L - \rho_0}{\rho_0} \times 100\%, \tag{1}$$

where R is the material's electrical resistance (Ω), l is the electrode interval (m), A is the electrode area (m^2), and ρ_0 is the initial electrical resistivity (Ω·m), and ρ_L is the electrical resistivity during flexural loading (Ω·m).

The self-sensing ability of MWCNT-reinforced ECCs was investigated under three loading scenarios: (1) continuous flexural loading: the specimen was continuously loaded at a constant rate of 0.5 mm/min until failure; (2) multiple-stage loading: the specimen was loaded at five stages. For each stage, the flexural load was applied at 0.5 mm/min for 1 minute and then kept the deflection constant for one more minute; (3) cyclic flexural loading: the flexural load was applied and released four times until reaching the specified midspan deflection. The specimen was dried under 60°C in the oven for two days to eliminate the effect of moisture.

3. Results and Discussion

3.1. Mechanical Properties. As shown in Figure 4, the ECC exhibits strain hardening behavior under both loading conditions. The strain first increased almost linearly with stress before the first cracking, which is the defined as the first inflection point. After that, more cracks developed, resulting in the plastic strain at increasing stress. The effect of MWCNTs on the first cracking strength, first cracking strain or deflection, ultimate strength, and ultimate strain or deflection was discussed in the following section.

Figure 5 shows the effect of MWCNT type and dosage on the uniaxial tensile properties. Figure 5(a) shows that the first cracking strength increased with the increase of MWCNT dosage. The specimens with different MWCNTs had similar strength. The first cracking strength increased by 18.2%, 34.8%, 40.3%, and 45.9%, as the MWCNTa dosage increased from 0 to 0.1%, 0.3%, 0.5%, and 0.7%, respectively. When MWCNTb was added, the first cracking strength increased by 8.8%, 26.0%, 33.1%, and 43.1%, respectively. Figure 5(b) indicates that when MWCNT content increased from 0% to 0.7%, the ultimate tensile strength for the ECC with MWCNTa increased by 6.2%, 11.7%, 23.1%, and 31.7%, respectively, and for the ECC with MWCNTb, the ultimate tensile strength increased by 3.8%, 9.0%, 20.7%, and 33.1%, respectively. These two types of MWCNTs had a similar effect on ultimate tensile strength. The increase of strength by adding MWCNTs could be possibly caused by several reasons. First, MWCNTs could act as the filler inside the skeleton of hardened cement paste, resulting in denser structure. Second, MWCNTs could accelerate early-age cement hydration. Third, MWCNTs are able to bridge the microcracks due to its very high length to diameter ratio [20, 26].

Different from strength, the first cracking and ultimate tensile strains decreased as MWCNTs were added. As shown in Figure 5(c), when MWCNT content increased from 0% to 0.7%, the first cracking tensile strain reduced 6.3%, 25.0%, 34.4%, and 25.0% for the MWCNTa-ECC, and by 25.0%, 31.3%, 40.6%, and 12.5% for the MWCNTb-ECC,

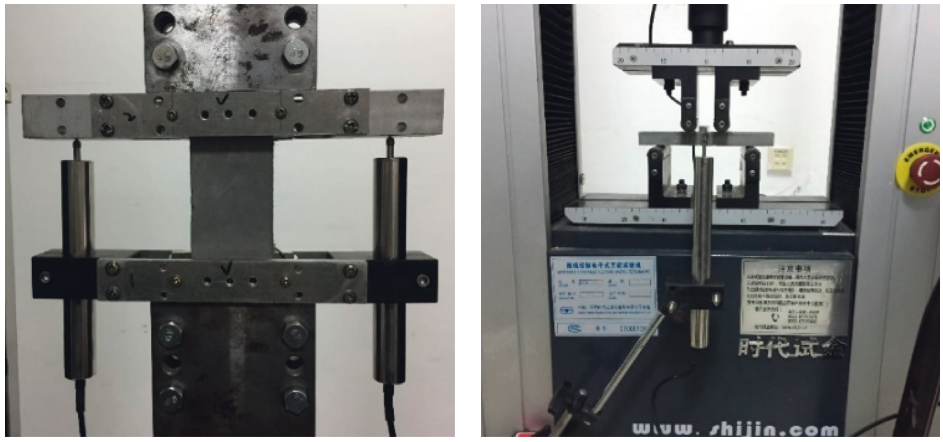

(a) (b)

Figure 2: Testing setups for mechanical behavior: (a) uniaxial tensile test and (b) four-point bending test.

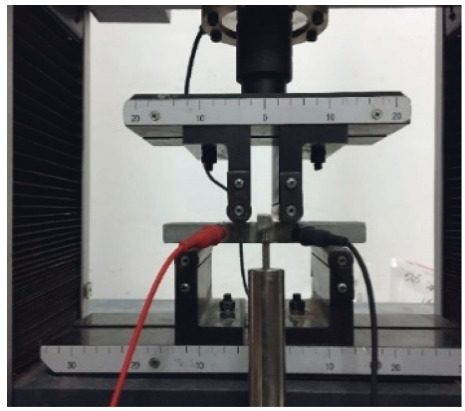

Figure 3: Testing setup for electrical resistivity of the ECC.

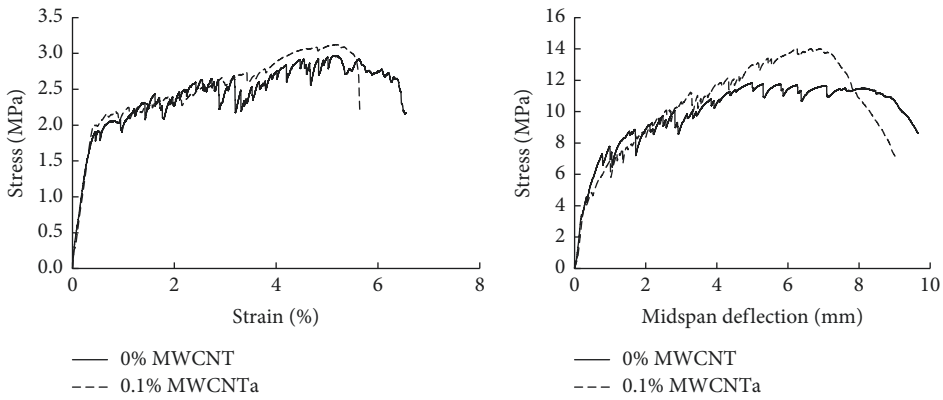

(a) (b)

Figure 4: Typical mechanical behavior of different ECC mixes. (a) Uniaxial tensile stress-strain curve. (b) Midspan deflection under flexural loading.

respectively. The reduction could be caused by the increased modulus and also the bridging effect of MWCNTs, which limits the deformation of the ECC matrix when the ECC starts to crack. The reduction of ultimate tensile strain was higher than that of the first cracking strain. The ultimate tensile strain was decreased by 13.7%, 25.1%, 30.0%, and 27.6% for the MWCNTa-ECC and by 4.5%, 15.9%, 21.5%, and 20.1% for the MWCNTb-ECC, respectively. The reduction of the ultimate tensile strain could be caused by the improved fiber-to-matrix bond.

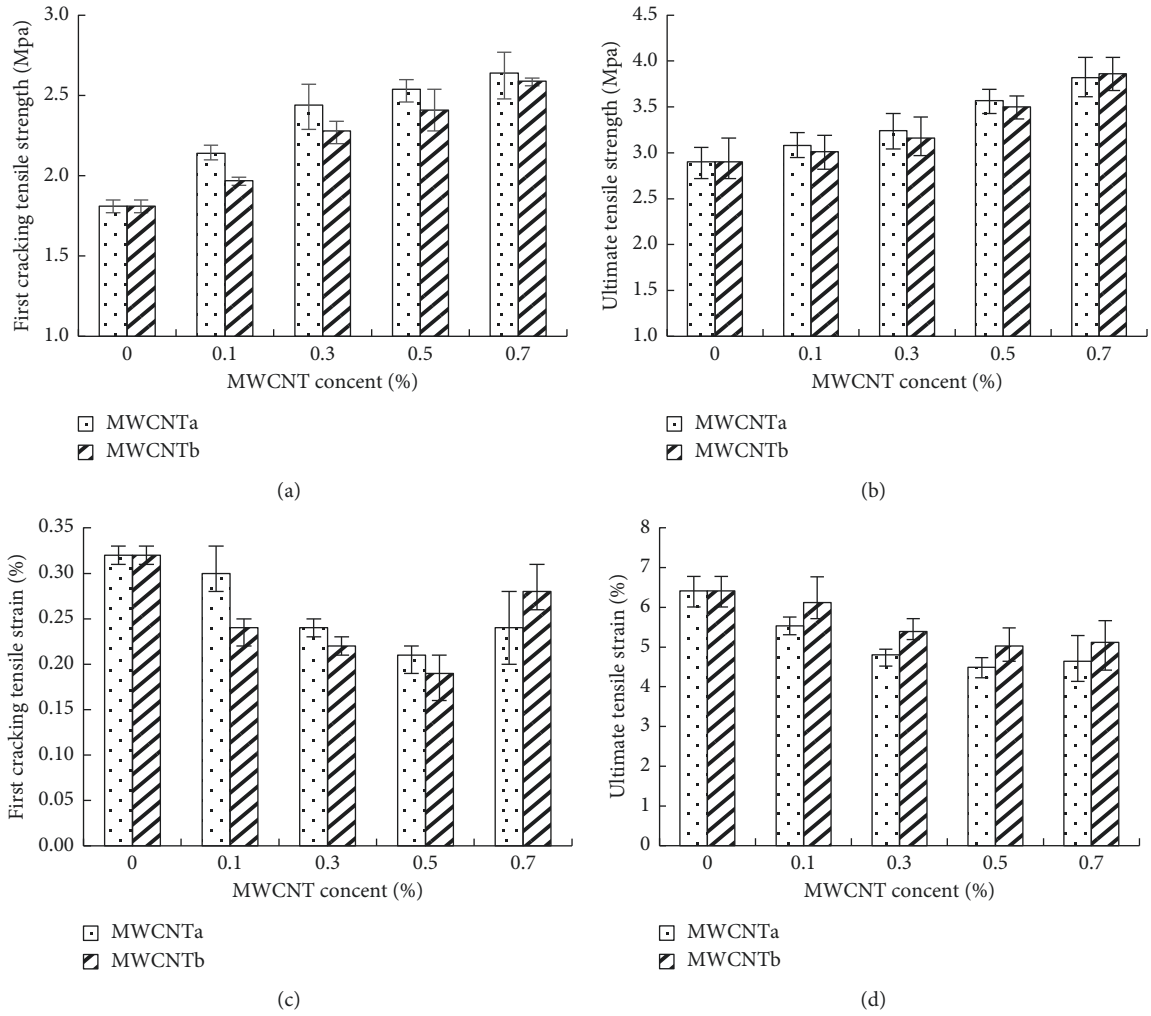

Figure 5: Characteristics of stress-strain curves of the uniaxial tensile test for MWCNT-reinforced ECCs. (a) First cracking tensile strength. (b) Ultimate tensile strength. (c) First cracking tensile strain. (d) Ultimate tensile strain.

Figure 6 shows the flexural behavior of ECCs with different dosages and types of MWCNTs. As shown in Figure 6(a), MWCNTs had significant effect on the first cracking flexural strength, which increased as the dosage of MWCNTs increased. When MWCNT content increases from 0% to 0.7%, the strength increased by 78.2%, 94.0%, 130.9%, and 125.6% for the MWCNTa-ECC and by 77.7%, 81.4%, 97.2%, and 105.3% for the MWCNTb-ECC. However, MWCNTs had less effect on ultimate flexural strength (Figure 6(b)). When MWCNT content increases from 0% to 0.7%, the ultimate flexural strength increased 17.2%, 22.1%, 27.3%, and 22.6%, respectively, for the MWCNTa-ECC and 12.8%, 19.0%, 4.1%, and 28.4%, respectively, for the MWCNTb-ECC. This trend is consistent with current research [28]. As observed by Sakulich and Li [28], CNTs consolidated around the PVA fibers and could increase mechanical properties by bridging microcracks. Therefore, the first cracking strength increased. Different from the first cracking strength, the ultimate flexural strength depends more on fiber-to-matrix bonding and the matrix's elastic modulus [29, 30]. MWCNTs may form a strong matrix-to-CNT bond, but the effect could be reduced by the improved matrix density and stiffness [27].

Similar to the tensile strain, MWCNTs reduced the midspan first cracking and ultimate deflection. As shown in Figure 6(c), the MWCNTa-ECC had higher midspan first cracking deflection than the MWCNTb-ECC, except when 0.7% MWCNTs was added. The MWCNTa-ECC, however, had lower ultimate deflection than the MWCNTb-ECC. The highest reduction of ultimate deflection was 41.1% and 22.0% for the MWCNTa-ECC and MWCNTb-ECC, respectively.

3.2. Self-Sensing Behavior. Figure 7 shows that the addition of MWCNTs, regardless of the type of MWCNTs, reduced the electrical resistivity. As the dosage of MWCNTs increased from 0.1% to 0.3%, the resistivity was reduced around 54% for both types of ECCs. After that, the resistivity started to decrease slowly with the increase of MWCNTs. The resistivity of the ECC was determined by

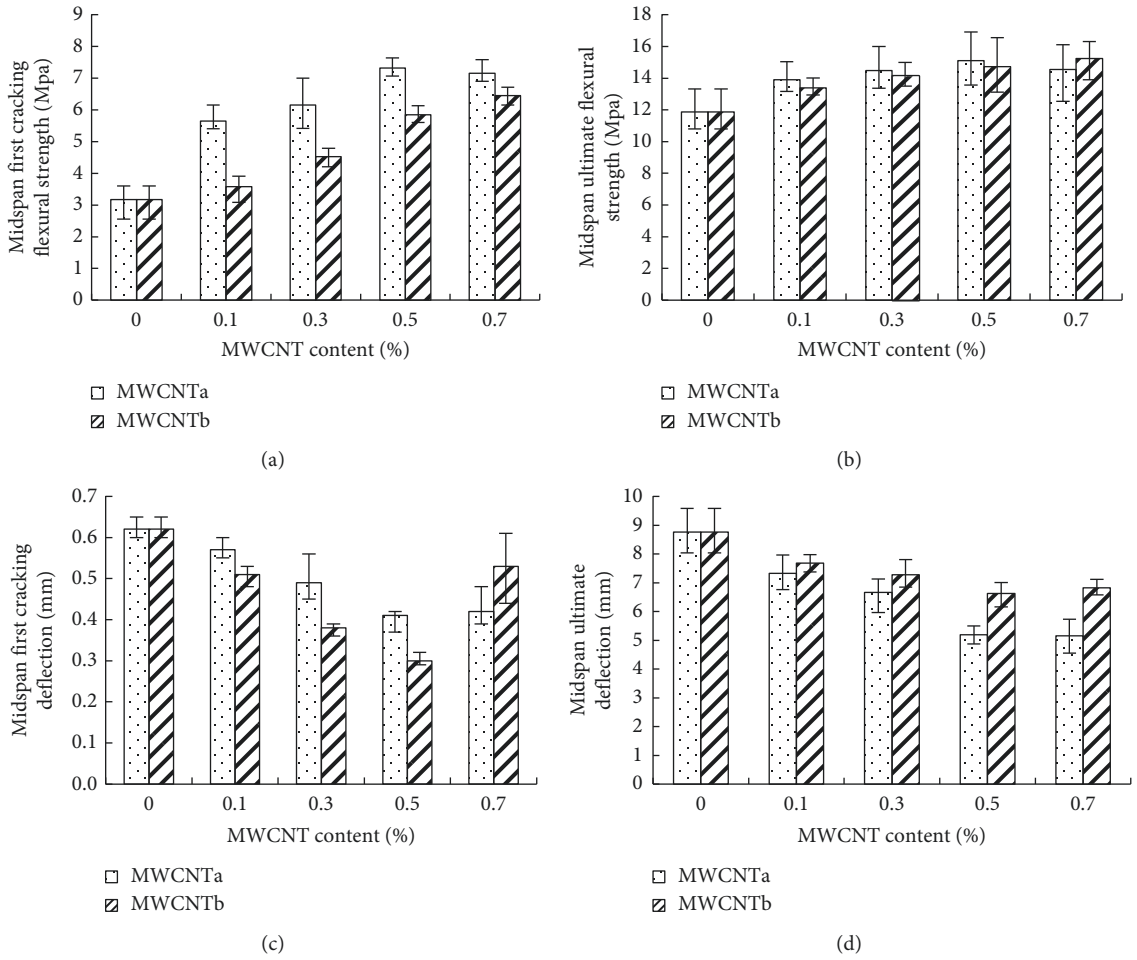

Figure 6: Stress-deflection curves of the flexural test for ECCs containing different MWCNTs. (a) First cracking flexural strength of MWCNT-ECCs. (b) Ultimate flexural strength of MWCNT-ECCs. (c) Midspan first cracking deflection of MWCNT-ECCs. (d) Midspan ultimate deflection of MWCNT-ECCs.

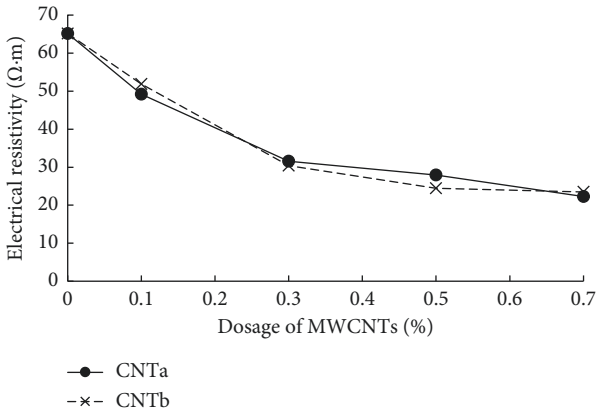

Figure 7: Electrical resistivity of ECCs containing different types of MWCNTs.

two aspects: (1) the intrinsic resistance of the cement matrix and MWCNTs and (2) the contact resistivity of MWCNTs, including resistance between the connected MWCNTs and the tunnelling resistance effect, which depends on the thickness and the conductive properties of the matrix filling the tunnelling gap [27]. As the dosage of MWCNTs increased, more and more MWCNTs are connected, resulting in lower contact resistance and smaller thickness of gaps among unconnected MWCNTs, which in turn reduces tunnelling resistance. Therefore, the resistivity of the ECC reduces with the increase of MWCNT dosage. When the connected MWCNT network is formed, the resistivity is mainly determined by direct contact resistivity of MWCNTs. Therefore, the further increase of MWCNTs will not significantly decrease the resistivity [22]. This phenomenon is called electrical percolation [31]. Figure 7 indicates that MWCNT-reinforced ECCs had typical features of electrical percolation phenomenon. The percolation threshold of ECCs containing MWCNTs was around 0.3% by weight, over which resistivity drops sharply. Since the type of MWCNTs had no significant effect on resistivity, the ECC with MWCNTa was selected to investigate the self-sensing behavior.

Figure 8 illustrates the self-sensing behavior of ECCs with 0.3% MWCNTa subjected to continuous four-point flexural loading. As shown in the figure, the fractional change in resistivity (FCR) increased with time. The FCR

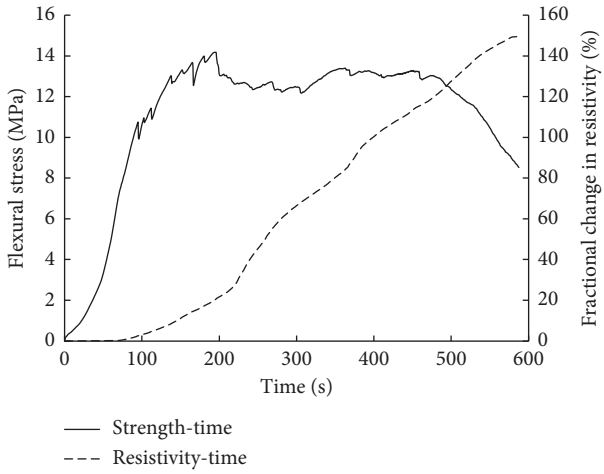

Figure 8: Self-sensing behavior of ECCs subjected to flexural loading.

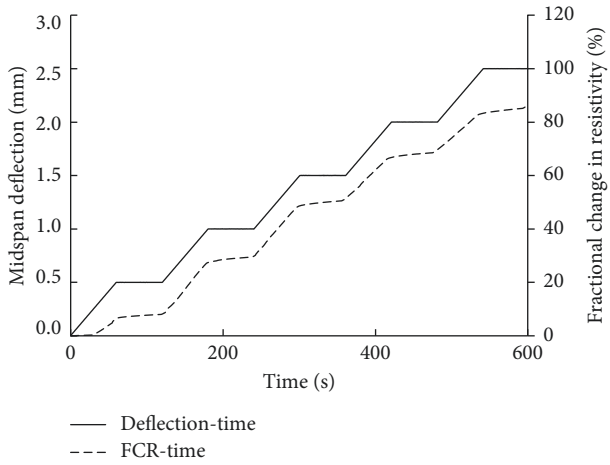

Figure 9: Self-sensing behavior of MWCNT-reinforced ECCs subjected to multiple-stage loading.

curve could be divided into two stages: before and after the first crack. Before the first crack, the FCR increased slowly. At this stage, as the stress increased, the distance among MWCNTs increased and some connected MWCNTs were separated, resulting in higher resistivity [26, 27]. After the first crack, multiple cracks developed and crack width increased. The cracks cut off some electric channels, resulting in much higher resistivity. Therefore, FCR increases quickly. Figure 9 shows the self-sensing behavior of ECCs subjected to multiple-step loading. The FCR changed simultaneously with the deflection. The FCR was constant when the deflection was kept unchanged. The FCR was over 80% when the deflection increased to 3.5 mm. According to Figures 8 and 9, ECCs with MWCNTs had good self-sensing ability.

Figure 10 illustrates the self-sensing behavior of ECCs containing 0.3% MWCNTa under cyclic loading at different midspan deflection ranges. Generally, the resistivity increased upon loading and decreased upon unloading in every cycle. When the midspan deflection was between 0.1 and 0.6 mm, the resistivity was also reversible, indicating better self-sensing ability. When the midspan deflection was less than 0.2 mm, specimen was under elastic stage without no apparent cracks. During this stage, the change of resistivity was mainly caused by the separation of MWCNTs, leading to higher contact resistivity. When the defection reached 0.6 mm, the specimen was in the plastic range and cracks were formed. The change of resistivity was mainly caused by crack opening and closing. As shown in the figure, FCR reached 9% when the deflection was from 0.1 to 0.6 mm.

Figure 11 indicates that the dosage of MWCNTs had significant effect on the self-sensing ability. For MWCNT content up to 0.7%, the FCR had good relationship with the midspan deflection. However, as the MWCNT content increased, the amplitude of FCR decreased. The FCR decreased from 9% to 4.1% and 2.5% when the dosage of MWCNTs increased from 0.3% to 0.5% and 0.7%, respectively. This could be caused by the MWCNT network inside ECCs. As the MWCNT content increased, the tunnelling gap would be shortened, and then the MWCNT network was getting stabilized and hard to change under loading, resulting in lower FCR.

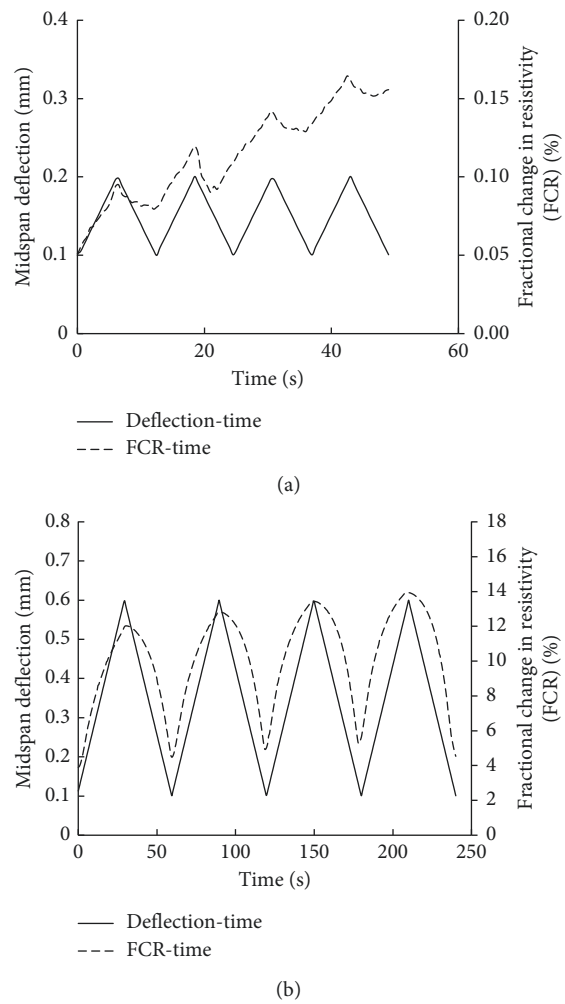

Figure 10: Self-sensing behavior of MWCNT-reinforced ECCs subjected to cyclic flexural loading. (a) 0.1-0.2 mm. (b) 0.1–0.6 mm.

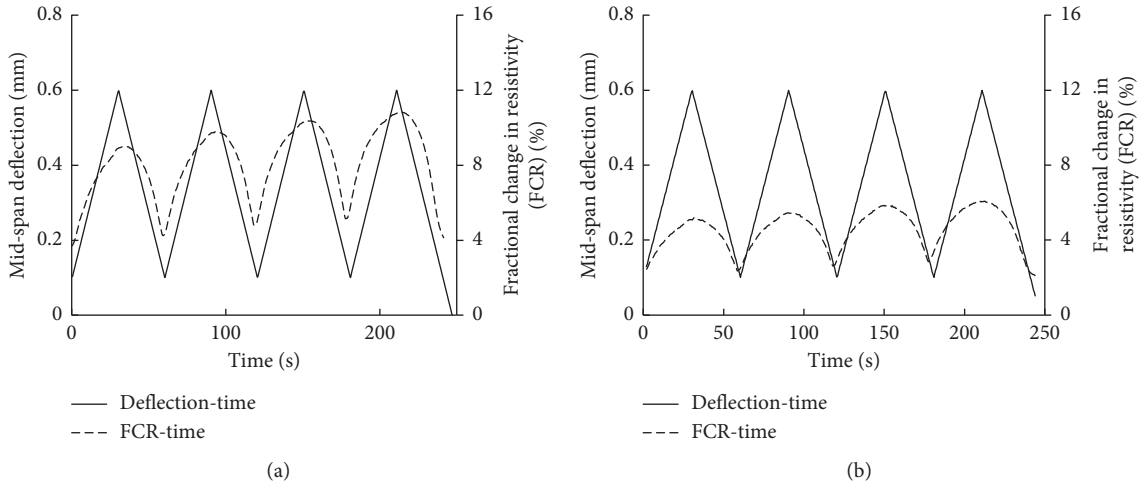

Figure 11: Effect of dosage of MWCNTs on the self-sensing ability: (a) 0.5% MWCNT and (b) 0.7% MWCNT.

4. Conclusions

This paper studied the mechanical and self-sensing properties of MWCNT-reinforced ECCs. The conclusions are listed as follows:

(1) MWCNTs improved first cracking tensile strength and ultimate tensile strength under the uniaxial tensile test while reducing first cracking tensile strain and ultimate tensile strain. For the four-point flexural testing, MWCNTs improved first cracking flexural strength and ultimate flexural strength, while reducing midspan first cracking deflection and midspan ultimate deflection.

(2) The percolation threshold of ECCs containing MWCNTs was around 0.3% by weight.

(3) ECCs containing MWCNTs had good self-sensing ability under both continuous flexural loading, multiple-step loading, and cyclic loading conditions. When the midspan deflection was between 0.1 and 0.6 mm, the FCR reached 9%.

(4) The dosage of MWCNTs had significant effect on the self-sensing ability. As the MWCNT content increased, the amplitude of FCR decreased.

Data Availability

The data used to support the findings of this study are included within the article.

Conflicts of Interest

The authors declare that there are no conflicts of interest regarding the publication of this paper.

Acknowledgments

This study was supported by the National Natural Science Foundation of China (51108247 and 51478252), Key Research and Development Program of Shandong Province (2015GSF122009), and Natural Science Foundation of Shandong Province (ZR2016EEM03).

References

[1] W. A. Li, "Method for structural safety monitoring of composite carbon fiber reinforced concrete," *China Safety Science Journal*, vol. 15, pp. 109–112, 2015.

[2] Z. Ge, D. Wang, R. Sun, and M. Oeser, "Einsatz von kohlenstoffnanoröhren im straßenbeton zur selbstüberwachung," *Bautechnik*, vol. 92, no. 3, pp. 189–195, 2015.

[3] B. Han, S. Sun, S. Ding, L. Zhang, X. Yu, and J. Ou, "Review of nanocarbon-engineered multifunctional cementitious composites," *Composites Part A: Applied Science and Manufacturing*, vol. 70, pp. 69–81, 2015.

[4] G. Y. Li, P. M. Wang, and X. Zhao, "Mechanical behavior and microstructure of cement composites incorporating surface-treated multi-walled carbon nanotubes," *Carbon*, vol. 43, no. 6, pp. 1239–1245, 2005.

[5] B. Han, X. Yu, E. Kwon, and J. Ou, "Effects of CNT concentration level and water/cement ratio on the piezoresistivity of CNT/cement composites," *Journal of Composite Materials*, vol. 46, no. 1, pp. 19–25, 2012.

[6] J. L. Luo, Z. D. Duan, T. J. Zhao, and Q. Y. Li, "Effect of compressive strain on electrical resistivity of carbon nanotube cement-based composites," *Key Engineering Materials*, vol. 483, pp. 579–583, 2011.

[7] A. Yazdanbakhsh, Z. Grasley, B. Tyson, and R. Abu Al-Rub, "Challenges and benefits of utilizing carbon nanofilaments in cementitious materials," *Journal of Nanomaterials*, vol. 2012, Article ID 371927, 8 pages, 2012.

[8] D. D. L. Chung, "Piezoresistive cement-based materials for strain sensing," *Journal of Intelligent Material Systems and Structures*, vol. 13, no. 9, pp. 599–609, 2002.

[9] G. Yıldırım, M. H. Sarwary, A. Al-Dahawi, O. Öztürk, A. Özgür, and M. Şahmaran, "Piezoresistive behavior of CF- and CNT-based reinforced concrete beams subjected to static flexural loading: shear failure investigation," *Construction and Building Materials*, vol. 168, pp. 266–279, 2018.

[10] A. Al-Dahawi, O. Öztürk, F. Emami, G. Yıldırım, and M. Şahmaran, "Effect of mixing methods on the electrical

properties of cementitious composites incorporating different carbon-based materials," *Construction and Building Materials*, vol. 104, pp. 160–168, 2016.

[11] V. C. Li, "On engineered cementitious composites (ECC)," *Journal of Advanced Concrete Technology*, vol. 1, no. 3, pp. 215–230, 2003.

[12] V. C. Li, C. Wu, S. Wang et al., "Interface tailoring for strain-hardening polyvinyl alcohol-engineered cementitious composites (PVA-ECC)," *ACI Materials Journal*, vol. 99, no. 5, pp. 463–472, 2002.

[13] H. Q. Xue and Z. C. Deng, "Study on durability of engineered cementitious composites," *Advanced Materials Research*, vol. 236–238, pp. 2688–2693, 2011.

[14] M. Şahmaran and V. C. Li, "Durability of mechanically loaded engineered cementitious composites under highly alkaline environments," *Cement and Concrete Composites*, vol. 30, no. 2, pp. 72–81, 2008.

[15] X. Huang, R. Ranade, W. Ni, and V. C. Li, "Development of green engineered cementitious composites using iron ore tailings as aggregates," *Construction and Building Materials*, vol. 44, pp. 757–764, 2013.

[16] J. Yu, J. Lin, Z. Zhang, and V. C. Li, "Mechanical performance of ECC with high-volume fly ash after sub-elevated temperatures," *Construction and Building Materials*, vol. 99, pp. 82–89, 2015.

[17] M. Şahmaran, E. Özbay, H. E. Yücel, M. Lachemi, and V. C. Li, "Frost resistance and microstructure of engineered cementitious composites: influence of fly ash and micro poly-vinyl-alcohol fiber," *Cement and Concrete Composites*, vol. 34, no. 2, pp. 156–165, 2012.

[18] M. Sahmaran and V. C. Li, "Durability properties of micro-cracked ECC containing high volumes fly ash," *Cementitious Concrete Research*, vol. 39, no. 11, pp. 1033–1043, 2009.

[19] B. Han, X. Yu, and J. Ou, "Multifunctional and smart carbon nanotube reinforced cement-based materials," *Nanotechnology in Civil Infrastructure*, pp. 1–47, 2011.

[20] V. W. J. Lin, M. Li, J. P. Lynch, and V. C. Li, "Mechanical and electrical characterization of self-sensing carbon black ECC," vol. 7983, pp. 1–12, 2011.

[21] A. Al-Dahawi, M. H. Sarwary, O. Öztürk et al., "Electrical percolation threshold of cementitious composites possessing self-sensing functionality incorporating different carbon-based materials," *Smart Materials and Structures*, vol. 25, no. 10, pp. 1–15, 2016.

[22] A. Al-Dahawi, G. Yıldırım, O. Öztürk, and M. Şahmaran, "Assessment of self-sensing capability of engineered cementitious composites within the elastic and plastic ranges of cyclic flexural loading," *Construction and Building Materials*, vol. 145, no. 1, pp. 1–10, 2017.

[23] S. Kumar, P. Kolay, S. Malla, and S. Mishra, "Effect of multiwalled carbon nanotubes on mechanical strength of cement paste," *Journal of Materials in Civil Engineering*, vol. 24, no. 1, pp. 84–91, 2012.

[24] B. M. Tyson, R. K. Abu Al-Rub, A. Yazdanbakhsh, and Z. Grasley, "A quantitative method for analyzing the dispersion and agglomeration of nano-particles in composite materials," *Composites Part B: Engineering*, vol. 42, no. 6, pp. 1395–1403, 2011.

[25] M. Li and V. C. Li, "Rheology, fiber dispersion, and robust properties of engineered cementitious composites," *Materials and Structures*, vol. 46, no. 3, pp. 405–420, 2013.

[26] M. A. Etman, S. S. Shebl, A. A. Mosallam, and M. A. EL-Dimerdash, "Effect of carbon nanotubes addition on mechanical properties of cement paste," *HBRC Journal*, vol. 7, no. 1, pp. 1–8, 2011.

[27] K. Gopalakrishnan, B. Birgisson, P. Taylor, and N. O. Attoh-Okine, *Nanotechnology in Civil Infrastructure*, Springer, Berlin, Germany, 2011.

[28] A. R. Sakulich and V. C. Li, "Nanoscale characterization of engineered cementitious composites (ECC)," *Cement and Concrete Research*, vol. 41, no. 2, pp. 169–175, 2011.

[29] H. Siad, M. Lachemi, M. Sahmaran, H. A. Mesbah, and K. A. Hossain, "Advanced engineered cementitious composites with combined self-sensing and self-healing functionalities," *Construction and Building Materials*, vol. 176, pp. 313–322, 2018.

[30] M. S. Sahmaran, H. E. Yücel, S. Demirhan, and C. V. Li, "Combined effect of aggregate and mineral admixtures on tensile ductility of engineered cementitious composites," *Journal of ACI Material*, vol. 109, no. 6, pp. 627–638, 2012.

[31] P. Xie, P. Gu, and J. J. Beaudoin, "Electrical percolation phenomena in cement composites containing conductive fibres," *Journal of Materials Science*, vol. 31, no. 15, pp. 4093–4097, 1996.